A copper activated protease regulates photosynthetic soluble electron carriers in cyanobacteria

Raquel García-Cañas[1,2], Joaquín Giner-Lamia[2,3], Francisco J. Florencio[1,2] and Luis López-Maury*[1,2].

1. Instituto de Bioquímica Vegetal y Fotosíntesis, Universidad de Sevilla- CSIC, c/Américo Vespucio 49, 41092 Sevilla, Spain.

2. Departamento de Bioquímica Vegetal y Biología Molecular, Facultad de Biología, Universidad de Sevilla, Avenida Reina Mercedes s/n, 41012 Sevilla, Spain

3. Present address: Centro de Biotecnología y Genómica de Plantas UPM – INIA Parque Científico y Tecnológico de la U.P.M. Campus de Montegancedo, Autopista M-40, Km 38, Pozuelo de Alarcón, Madrid 28223, Spain

*To whom correspondence should be addressed:

Luis López-Maury, Instituto de Bioquímica Vegetal y Fotosíntesis, Telephone: +34 954489500; E-Mail: llopez1@us.es

Keywords: *Synechocystis*, metal homeostasis, plastocyanin, cytochrome c_6, photosynthesis

Abstract

After the GEO iron availability was greatly reduced and photosynthetic organisms evolved several alternative proteins. One of these proteins is plastocyanin, a type I blue-copper protein able to replace cytochrome-c_6 as soluble electron carrier between cytochromeb_6f and PSI. In most cyanobacteria, expression of these two alternative proteins is regulated by copper availability but the regulatory system remained unknown. Here we show that the regulatory system is composed by a BlaI/CopY family transcription factor (PetR) that represses *petE* (plastocyanin) expression and activates *petJ* (cytochrome-c_6) and a BlaR membrane protease (PetP) that regulates PetR. Using an *in vitro* assay, we show that PetP degrades PetR directly in the presence of copper. Transcriptomic analysis has revealed that PetRP system regulates only 4 genes (*petE*, *petJ*, *slr0601* and *slr0602*) highlighting its specificity. Even more, phylogenomic analysis suggest that *petE* and *petRP* acquisition could be an early adaptation to reduced iron bioavailability after GEO.

Introduction

Cyanobacteria are prokaryotes able to perform oxygenic photosynthesis and were responsible for the appearance of oxygen in the atmosphere. Although the timing of the Great Oxygenation Event (GEO) is well stablished, its extent is still a matter of dispute[1–4]. GEO caused a massive extinction as oxygen was toxic for most life forms [5,6] and provoked Fe oxidation (Fe^{2+} to Fe^{3+}), which made Fe much less available since Fe^{3+} precipitated. This created an additional problem for all forms of life because Fe was already stablished as the main cofactor in biochemical reactions[7,8]. In fact, photosynthesis has high Fe requirements and photosynthetic organisms usually have a higher Fe quota than non-photosynthetic organisms because Fe is contained in proteins of both photosystems, in the cytochrome b_6f complex, in the soluble thylakoid lumen electron carrier cytochrome c_6 ($Cytc_6$) and in ferredoxin outside thylakoid. Nowadays, Fe is a limiting nutrient in most ecosystems, especially in aquatic environments [9]. Consequently, photosynthetic organisms evolved several alternative proteins to iron-containing proteins. In most cyanobacteria and some algae, $Cytc_6$ can be replaced by plastocyanin (PC), a type I blue-copper protein that acts as thylakoid lumen soluble electron transporter. As these two electron carriers are known to be in the millimolar concentration range inside the thylakoid lumen[10], replacing $Cytc_6$ by PC substantially reduces the Fe requirement. In addition, PC uses Cu which is much more soluble (and therefore available) than Fe in an oxidising atmosphere. Interestingly, plants retained only PC and although a $Cytc_6$-like protein was identified it does not function work as photosynthetic electron carrier[11].

Expression of these two alternative electron carriers is regulated by copper availability in both cyanobacteria and algae[12–14]. The regulatory system has been well characterized in the green algae *Chlamydomonas reinhardtii*. CRR1, an SBP transcription factor, activates *CYC6* (encoding $Cytc_6$) expression in response to copper limitation[15]. CRR1 is able to bind both Cu^{+} and Cu^{2+} with the latter inhibiting DNA binding of SBP domain[16]. In contrast, this system is still unknown in cyanobacteria, despite the PC/$Cytc_6$ switch was discovered for more than 40 years [12,13,17–20] and frequently used for controlled expression of genes in several model systems[21–23]. The switch responds to the presence of copper at transcriptional level: *petJ* (encoding $Cytc_6$) is repressed while *petE* (encoding for PC) is induced [17,20,24–26]. Several regulatory systems that respond to copper have been described in cyanobacteria

(CopRS[24,26], InrS[25,26], BmtR[27]) but none of them are involved in regulating these two genes.

Here we unveil the regulatory mechanism for the PC/$Cytc_6$ switch in cyanobacteria. It is composed by two genes: one coding for a transcription factor of the BlaI superfamily (PetR) that binds to both *petE* and *petJ* promoters, repressing *petE* and activating *petJ* in the absence of copper. The second gene codes for a protease (PetP) that degrades PetR in response to copper. PetP is activated by copper both *in vivo* and in an *in vitro* assay system, suggesting that it works as the sensor of the system. The widespread presence of this regulatory system in cyanobacteria (which includes early branching cyanobacteria such as *Gloeobacter*) suggests that its acquisition occurred early in the evolution probably as adaptation to reduced iron availability after GEO.

Materials and Methods

Strains and culture conditions.

All *Synechocystis* strains used in this work were grown photoautotrophically on BG11C or BG11C-Cu (lacking $CuSO_4$) medium at 30º C under continuous illumination (50 µmol photon m^{-2} s^{-1}) and bubbled with a stream of 1% (v/v) CO_2 in air. BG11C-Cu was supplemented with 300 µM BCSA as a chelating agent to trap any trace of copper, when required. For plate cultures, media was supplemented with 1% (wt/vol) agar. Kanamycin, nourseothricin, chloramphenicol, spectinomycin and erythromycin were added to a final concentration of 50 µg mL^{-1}, 50 µg mL^{-1}, 20 µg mL^{-1}, 5 µg mL^{-1} and 5 µg mL^{-1}, respectively. Experiments were performed using cultures from the logarithmic phase (3-4 µg chlorophyll mL^{-1}). *Synechocystis* strains are described in Table 1.

E. coli DH5α cells were grown in Luria Broth or M9 (supplemented with 1mL LB per L of M9) media and supplemented with 100 µg mL^{-1} ampicillin, 50 µg mL^{-1} kanamycin, 50 µg mL^{-1} nourseothricin, 20 µg mL^{-1} chloramphenicol and 100 µg mL^{-1} spectinomycin when required.

Insertional mutagenesis of Synechocystis genes.

For slr0240 (*petR*) mutant construction a 1524 pb was amplified using oligonucleotides 223 and 224 cloned in pSPARKII (generating pPETR) and a Sp^R cassette was inserted in the *Eco*RV site at 31st codon in the *slr0240* ORF generating plasmid pPETR_Sp. For slr0241 (*petP*) mutant a 970 pb was amplified using oligonucleotides 248-249 and cloned into pSPARKII generating pPETP. A 582 pb *Nhe*I fragment was substituted by an *Xba*I erythromycin cassette generating pPETP_Ery. For the *petRP* double mutant a 1492 pb fragment was amplified by PCR using oligonucleotides 256-257 and cloned into pSPARKII vector generating pPETRP plasmid. A 650 pb *Bst*EII fragment form plasmid pPETRP was substituted by an *Hinc*II digested SpR cassette from pRLSpec generating pPETRP_Sp. To generate a *petJ* mutant a 1023 pb DNA fragment was amplified using oligos 235-236 and cloned into pSPARKII generating pPETJ and a *Xba*I CC1 Cm resistance cassette was inserted in the *Nhe*I site present in *petJ* ORF generating pPETJ_Cm. These plasmids were used to transform WT *Synechocystis*, PETE or PETJ strains generating PETR, PETP and PETRP, PETER, PETEP, PETERP, PETJR, PETJP, PETJRP and PETEJ strains. Segregation of the strains was verified by PCR with the appropriate primer pairs as depicted in figures 7 and S2. All plasmids were sequenced to verify that no mutations were introduced. Sequences for all oligonucleotides are shown in Table S1.

RNA isolation and Northern-blot analysis

Total RNA was isolated from 30 mL samples of *Synechocystis* cultures in the mid-exponential growth phase (3 to 4 µg chlorophyll m L^{-1}). Extractions were performed by vortexing cells in presence of phenol-chloroform and acid-washed baked glass beads (0.25-0.3 mm diameter) as previously described [28]. 5 µg of total RNA was loaded per lane and electrophoresed in 1.2 % agarose denaturing formaldehyde gels[29] and transferred to nylon membranes (Hybond N-Plus; GE Healthcare). Prehybridization, hybridization, and washes were in accordance with GE Healthcare instruction manuals. Probes for Northern blot hybridization were synthesized by PCR using oligonucleotide pairs: 172-173, 174-175, 389-390, 275-276, 274-275 and 178-179 (see Table S1) for *petE*, *petJ*, *copM*, *slr0601* and *rnpB* respectively. DNA probes were ^{32}P labelled with a random-primer kit (Rediprime II catalog #RPN1633, GE biosciences) using [α-32P] dCTP (3,000 Ci/mmol). Hybridization signals were quantified with a Cyclone Phosphor System (Packard). Each experiment was performed at least three biological independent times.

Western blotting.

For western blot analysis, proteins were fractionated on SDS PAGE and immunoblotted with antibodies against: plastocyanin (1:3,000), cytochrome c_6 (1:3,000), CopM (1:7,000), PetR (1:6,000) or *Synechococcus* sp. PCC 6301 glutamine synthetase I (1:100,000). The ECL Prime (catalog # RPN2232, GE biosciences) was used to detect the different antigens with anti-rabbit secondary antibodies conjugated to horseradish peroxidase (1:25,000; catalog # P8250, Sigma). Either photography films or ChemiDoc Imaging System Biorad (for quantification of signal) were used to detect the signals.

Samples were prepared from whole cells or soluble extracts. For whole cells 1 OD_{750nm} were collected, supernatant was carefully removed, cells were resuspended in 100 µl of 1X Laemmli loading buffer and boiled for 10 minutes. For soluble extracts 20 OD_{750nm} were resuspended in 300 µl of buffer A (50 mM Tris HCl pH 8, 50 mM NaCl, 1 mM PMSF) and broken using glass beads and two cycles of 1 min in a minibead-beater separated by 5 min on ice. Cell extracts were recovered from the beads and samples were clarified by two sequential centrifugations: 5 min at 5000 *g* to eliminate cells debris and 15 min at 15 000 *g* to remove membranes. Protein concentration in cell-free extracts or purified protein preparations were quantified using the Bradford reagent (catalog # 5000006, Bio-Rad), using ovalbumin as a standard and the specified amounts of proteins were separated on SDS–PAGE.

PetR Protein purification

The complete *petR* ORF was cloned from *Synechocystis* DNA after PCR amplification with oligonucleotides 233 and 234 and cloned into *Bam*HI-*Not*I pGEX6P generating pGEX_PETR. GST-PetR fusion protein was expressed in *E. coli* DH5α. 1 L of culture was grown in Luria broth medium to an optical density at 600 nm of 0.6, cooled to 4 ºC, 0.1 mM isopropyl-b-D-thiogalactopyranoside (IPTG) was added and culture was further grown at 25 ºC overnight. Cells were harvested by centrifugation, and resuspended in 5 mL of PBS buffer (150 mM NaCl, 16 mM Na_2HPO_4, 4 mM NaH_2PO_4, 4 mM phenylmethylsulfonyl fluoride, 7 mM β-mercaptoethanol) supplemented with 0.1% Triton X-100, broken by sonication on ice, and insoluble debris were pelleted by centrifugation 45 minutes 25000 *g*. Soluble extracts were mixed with 1 mL of glutathione agarose beads (catalogue number # 17075601, GE Healthcare) and incubated for 2 h at 4 ºC with gentle agitation. Then beads were transferred to a column and washed extensively with PBS buffer (20-30 column volumes) until no more protein was eluted from the column. Column was equilibrated with 10 volumes of 50 mM Tris HCl pH 7.5 150 mM NaCl 1 mM EDTA 1 mM DTT and the beads resuspended in 2 volumes of the same buffer. 20 µl of Precission protease (2 U/µL; catalogue # 27084301, GE Healthcare) were added and the beads were incubated overnight at 4º C. The beads were poured on an empty column and the flow through fraction was collected. This fraction was diluted three times in 50 mM Tris HCl pH 8 and applied to an hiTrap Heparin column (catalogue # 17040601, GE healthcare) connected to an Amersham FPLC system. The column was washed with 10 volumes of 50 mM Tris HCl 100 mM NaCl and a 20 ml gradient from 0.1-1M NaCl was applied. Fractions containing PetR were pooled and concentrated. GST-PetR fusion protein was eluted from glutathione agarose beads with 3 mL of 50 mM Tris HCl pH 8 containing 10 mM of reduced glutathione after washing the column with PBS.

Protease assays.

20 OD_{750nm} of the different *Synechocystis* strains were collected and resuspended in 300 µL of buffer containing 50 mM Tris-HCl pH 8, 50 mM NaCl, 10 % glycerol and 1 mM $ZnSO_4$ and broken with 2 volumes of glass beads using a minibeadbeater. Total cell-extracts were collected from the tube by piercing the bottom of the tubes with a needle. Extract were centrifuged for 5’ at 5000 *g* to remove the remaining glass beads and unbroken cells and the supernatant constituted the total extract. 2 µg of GST-PetR were added to 150 µL of total extracts (containing 150 µg of total protein) and incubated at 30 ºC. At the indicated times 20 µL were removed, mixed with 7 µL of 4X

Laemmli buffer and boiled for 10'. 5 µL were used for western blot analysis using α-PetR antibodies. For *E. coli* assays DH5α transformed with pN_petRP_Nat or pN_Nat were grown to late exponential phase (OD_{595nm} 1-2) and 20 OD_{595nm} were collected and processed in identical way as for *Synechocystis*. pN_petRP_Nat was constructed by excising a 1478 pb from pPETRP using *Eco*RI and *Xho*I, containing petRP and 185 pb upstream from *petR* ATG, and inserting it in pN_Nat [30] cut in the same way.

Band shift assay. Gel retardation assays.

Probes were PCR-synthesized using oligonucleotides 53-92 for *petE* promoter (217 pb), 299-262 for *petJ* promoter (103 pb), and 295-296 for *slr0601* (177 pb) which introduce a *Sal*I restriction sites in all cases. The resulting DNA was digested with *Sal*I and end-labelled with [α-32P]-dCTP (3000 Ci $mmol^{-1}$) using Sequenase v2.0 (Affymetrix Product # 70775Y). The binding reaction was carried out in a final volume of 20 µl containing 4 ng of labelled DNA and 4 µg salmon sperm DNA in 20 mM Tris HCl (pH 8.0), 150 mM KCl, 10 mM DTT, 1 mM EDTA, 10 % glycerol and different amounts (from 0.001 µg to 1 µg) of purified PetR. The mixtures were incubated for 30 min at RT and loaded on a TBE non-denaturing 6% polyacrylamide gel (acrylamide:bisacrylamide 30:0.6). Electrophoresis was carried out at 4ºC and 200V in 0.25X TBE. Gels were transferred to a Whatman 3 MM paper, dried and autoradiographed using a Cyclone Phosphor System (Packard). Each experiment was performed at least three times with two independent PetR preparations.

RNA seq

The quantity and quality of total RNA were evaluated using RNA electropherograms (Agilent 2100 Bioanalyzer; Agilent Technologies, Santa Clara, CA, USA) and library construction of cDNA molecules was carried out using Illumina Kapa Stranded Total RNA with Ribo-Zero Library Preparation Kit. The generated DNA fragments (DNA library) were sequenced in the Illumina Hiseq 4000 platform, using 150bp paired-end sequencing reads. Sequencing was carried out by (STAB VIDA, Lda, Lisbon, Portugal). Reads were aligned against the NCBI genome sequence for *Synechocystis* (NC_000911.1, NC_005229.1, NC_005230.1, NC_005231.1 and NC_005232.1), using bowtie2 version 2.2.4[31]. Raw read counts were calculated using the HTSeq-count function from HTSeq framework 0.11.0[32]. The Bioconductor DESeq2 package from R software was used to detect differentially expressed genes[33]. An adjusted *P*-value of <0.01 was considered significant. For RNAseq density profiles data were normalized using BamCoverage function from DeepTools2 0.8.0 and visualized with Integrative

Genomics Viewer 2.3.6 (IGV). RNA-seq dataset is available at GEO accession GSE155385.

Phylogenomic analysis

16s RNA from 169 cyanobacterial genomes (Supplementary material S1; all completed genomes from NCBI and those included in[34]) were aligned with MUSCLE 3.8.31 and a Maximum Likelihood (ML) phylogeny was estimated with IQ-TREE 1.6.11[35] using the best fitting model (automatically selected by ModelFinder function) and selecting the phylogeny with the highest likelihood from those found among independent searches, and bootstrap of 1000. *petE, petJ, petR* and *petP* genes were searched using TBLASTN. Only hits with ≥50 % of query coverage and >25 % of identity were considered as homologues. Phylogenetic tree was displayed and edited with the Interactive Tree Of Life webtool iTOL v4[36].

Oxygen evolution

Oxygen evolution was measured in Clark-type oxygen electrode (Hansatech Chlorolab 2) using mid-logarithmic (OD_{750nm}= 0.8-1) cultures adjusted to OD_{750nm}=0.5 in BG11C or BG11C-Cu+BCSA media supplemented with 20 mM $NaHCO_3$ using white LED light.

Results

A BlaI/CopY homolog regulates *petJ*/*petE* switch in *Synechocystis*

Bioinformatics analysis of neighbourhood genes of *petE* and *petJ* genes in cyanobacterial genomes revealed that a transcription factor of the BlaI/CopY family (renamed PetR) was associated with *petJ* and/or *petE* genes in 13 genomes (Figure S1). Although the number of genomes with this gene association was low, correlation of these two regulatory genes with the presence of both *petE* and *petJ* was higher. In this regard, 75 % of genomes harboring *petE* and *petJ*, also displayed petR (and a linked gene coding for a BlaR homolog, see below; Figure S1) and was only present in those genomes that contains *petE* and *petJ* (Figure S1; with only two exceptions, *Kamptonema formosum* PCC 6407 and *Oscillatoria* sp. PCC 6506).This raised the possibility that *petR* could be related to the *petE*/*petJ* switch. In order to test this hypothesis, a mutant in the *slr0240* gene coding for this transcription factor in *Synechocystis* was generated (PETR strain). The mutant strain fully segregated (Figure S2) and the phenotype was indistinguishable from the WT in BG11C plates (see below). Expression of *petJ* and *petE* genes was analysed by Northern blot in both WT and PETR strains after copper addition to BG11C-Cu grown cells. In WT cells, *petE* was induced in response to copper and *petJ* was repressed (Figure 1a), as previously described[17,24–26]. In contrast, in the PETR strain *petE* was expressed even in the absence of copper and *petJ* was not expressed in any condition (Figure 1a). On the other hand, *copM* expression, which is induced in response to copper[24,37], was similar in both strains. At protein levels, PC was induced in WT cells upon copper addition while $Cytc_6$ abundance decreased after 4 and 24 h. CopM levels increased after copper treatment with the unprocessed form of the protein accumulating first and the processed one at later time points (Figure 1b). In contrast, in the PETR strain $Cytc_6$ was not detected in any condition and PC was detected even in BG11C-Cu (Figure 1b). An increase in PC levels was still evident in the PETR strain after copper addition (Figure 1b), probably due to an increase in copper bound PC, which is more stable than apoPC[24,25], as mRNA levels did not change after copper addition (Figure 1a). No changes were detected in CopM induction pattern (Figure 1b). Similar results were obtained when protein levels were analysed in steady-state cells grown in media with different copper availabilities: PC was high in copper containing media, lower in BG11c-Cu and much lower in BG11c-Cu+BCSA (a copper specific chelator) in the WT strain (Figure 1c). The PETR strain expressed PC in all conditions but accumulated higher levels in copper containing media. Whereas $Cytc_6$ was not detected in the PETR

strain in any media, WT cells displayed higher levels in BG11c-Cu+BCSA than in BG11-Cu, being almost undetectable in copper containing media (Figure 1d).

Slr0241(PetP) is also involved in *petJ*/*petE* regulation

Immediately downstream to *petR* there is another gene (*slr0241* which we have named *petP*) that codes for a M48/M56 superfamily of proteases. *petP* start codon overlaps with the stop codon of *petR* and both genes were expressed as a single transcriptional unit (Figure S3). Furthermore, this organization is conserved in all cyanobacterial genomes containing these two genes (Figure S1), suggesting that both genes might be functionally related. To test this hypothesis, we generated a mutant in the *petP* gene. The mutant strain (PETP) was viable (Figure S2) and exhibited a similar growth phenotype to the WT in BG11C plates (see below). When gene expression was tested in this mutant, *petE* was repressed both in the presence and the absence of copper, while *petJ* was expressed constitutively (Figure 1a). The same results were observed at protein levels with $Cytc_6$ being detected both in the presence and the absence of copper, while PC was undetectable in any condition (Figure 1b). When the steady state proteins levels were analysed in different copper containing media, PC was not detected in any media in the PETP strain while $Cytc_6$ was detected in all media. Despite this, $Cytc_6$ levels were lower in copper containing media than in media lacking copper (Figure 1d). These data indicate that *petP* is involved in the regulation of both genes, acting in an opposite way to *petR*. A double mutant lacking both *petR* and *petP* genes was also generated (PETRP) (Figure S2). The PETRP strain showed the same phenotype as the PETR strain (Figure S4), revealing that *petP* acts upstream of *petR*.

PetP regulates PetR levels in response to copper

Given that PetP belongs to the M48/M56 superfamily of proteases this protein might regulate PetR by proteolysis. To investigate this hypothesis, we generated an antiserum against PetR that allowed us to monitor PetR protein abundance in response to copper. In the WT strain, PetR was detected in cells cultivated in BG11C-Cu and it was rapidly degraded after copper addition. Two bands were detected (15 kDa and ~12 kDa, Figure 2a), suggesting an initial and specific cut and later degradation of the fragments. In fact, in order to consistently detect PetR, whole cells were loaded on gels (see material and methods section) as PetR was quickly degraded during protein extract preparation. The best studied homologs of PetRP are BlaIR/MecIR proteins involved in antibiotic resistance from *Staphylococcus aureus* and *Bacillus licheniformis*

[38]. Processing of these proteins was initially identified in BlaI and it takes places after Phe100 residue, which is completely conserved in all cyanobacterial PetR (Figure S5). In fact, theorical molecular mass of the fragment generated by this digestion agreed with the expected size detected by western blot (Figure 2a and S5; expected sizes of the full-length and the processed protein are 15.80 and 12.38 kDa, respectively). In contrast to the WT strain, PetR levels did not change in response to copper in the PETP strain. (Figure 2). Therefore, the initial cleavage is probably mediated by PetP and the fragments are probably further degraded by other unspecific proteases. As expected, PetR was not detected in the PETR strain. When PetR protein abundance was analysed in steady state cultures grown in different copper regimes, its levels were clearly regulated in the WT strain, being higher in the presence of BCSA than in BG11-Cu and not detected in copper containing media (Figure 2 b and c). PetR level was higher in the PETP strain than in the WT strain, even when WT cells were cultured in the presence of BCSA, although it decreased slightly at higher copper availability (Figure 2 b and c). These data are in agreement with $Cytc_6$ and PC levels under the same conditions (Figure 1 c and d) and demonstrate that PetR protein abundance is regulated by PetP *in vivo* according to Cu availability.

PetP is a copper regulated protease that degrades PetR.

To further characterise this regulation, we used an *in vitro* degradation assay in which recombinant GST-PetR was incubated with total extracts from WT, PETR and PETP strains and then PetR processing was followed by western blot. GST-PetR was not degraded by whole cells extracts prepared from WT, PETP or PETR when copper was not added to the extracts (Figure 3a). In contrast, when copper was added to extracts GST-PetR was degraded by WT or PETR extracts, but not to PETP extracts, indicating that a PetP-mediated protease activity was activated by copper (Figure 3a). To confirm that PetP was directly involved in PetR degradation and that this degradation was not mediated by an additional protein from *Synechocystis*, *petRP* under their own promoter were cloned in a PBS derived plasmid and transformed into *E. coli*. Total extracts were prepared from cells carrying a plasmid containing *petRP* or an empty plasmid, and degradation of GST-PetR was monitored. The results were similar to what we observed in total extracts from *Synechocystis*: GST-PetR was degraded in total extracts prepared from cells containing a plasmid that includes *petRP* but not in extracts prepared from a strain carrying an empty plasmid (Figure 3b). PetR degradation also required copper supplementation of extracts, demonstrating that PetP is directly activated by this metal (Figure 3b). These results showed that PetP can degrade PetR

directly without the participation of any other protein from *Synechocystis*. Thus, PetP controls PetR levels directly by a copper dependent mechanism.

PetR binds to both *petE* and *petJ* promoters

In order to establish whether PetR regulates *petJ* and *petE* directly, we proceeded by using EMSA assays to analyse PetR binding to both promoter regions. As a first approach we carried out band shift assays using a recombinant version of PetR (see material and methods for details) and two probes corresponding to the *petJ* and *petE* promoters. PetR was able to bind to both promoters (Figure 4 a and b) and the binding was not affected by Cu (Cu^+ or Cu^{2+}; Figure S6). PetR showed a higher affinity towards *petE* than to the *petJ* promoter, being able to completely titrate the probe at lower concentrations (Figure 4a and b). These data point to a dual role of PetR activating *petJ* expression and repressing *petE*. In order to identify the PetR binding site, we carried out a bioinformatic analysis of the *petE* and *petJ* promoters in cyanobacterial genomes. 300 pb from *petE* and *petJ* promoters were retrieved from those genomes that contained *petE*, *petJ* and *petRP* using MGcV database (http://mgcv.cmbi.ru.nl/; Supplementary material S2). When the sequences from both *petE* and *petJ* promoters were analysed using MEME suite, the motif shown in Figure 4c was found significantly enriched in them. This motif contains the sequence GACN$_5$GTC completely conserved and it was found 75 pb upstream from the starting ATG codon (and 37 pb from the tsp) in the *petJ* promoter and at 118 pb from the ATG codon (and 23 pb from the tsp) in the *petE* promoter. In the *petJ* promoter, the putative binding site is centred around the -35 box in the promoter in a location suitable with an activator site. In contrast, this sequence is located between the -10 and the -35 boxes in the *petE* promoter, compatible with a repressor role of PetR. These locations are in agreement with our gene expression by northern blot (Figure 1) and transcriptomics analysis (see below) in PETR and PETP mutant strains, which suggests that PetR activates *petJ* and represses *petE* expression. Notably, when MEME analysis was repeated using only *petJ* promoters, an extended motif was identified (Figure 4d). This motif includes the core of motif shown in Figure 4c but also contained two direct repeats with the sequence TTTGAC-N$_9$-TTTGAC (Figure 4d). A different motif was also identified when the same analysis was performed using only *petE* promoter sequences (Figure 4e). This motif includes the core motif shown in Figure 4c but in an extended form of the inverted repeat GACA-N$_3$-TGTC. However, the *Synechocsytis* sequence in the *petE* promoter is GACG-N$_3$-TGTC (Figure 4f). These data suggest that binding of PetR to these two promoters might be in different configurations: inverted repeats in *petE*,

where it acts as a repressor, and both inverted and direct repeats in *petJ* to activate transcription. Binding to the *petJ* promoter could be mediated by a higher order complex as two dimers binding to both sides of DNA, generating a structure able to activate transcription. However, a single complex was detected after PetR binding to *petJ* although with lower affinity compared to *petE* promoter (Figure 4a and b).

RNAseq analysis of the PetR regulon

To fully characterise the PetR regulon, RNA seq was carried out using RNA extracted from WT, PETR and PETP strains grown in BG11C-Cu and 2 h after addition of 0.5 µM Cu. Using a cut off-of at least 2-fold change and P_{adj} <0.01, 14 genes were induced (*petE, copMRS* (both plasmid and chromosomal copies)*, copBAC and nrsBAC*) and 3 repressed (*petJ, slr0601, slr0602*) after copper addition in the WT strain (Table 2; Supplementary material S3 and S4), in agreement with previous microarray analysis[26]. A similar response was observed in the PETR strain with *copMRS* (both copies)*, copBAC* and *nrsBAC* operons and three additional genes of unknown function were also differentially regulated (Table 2). In the PETP strain 16 genes were induced after copper treatment, including *copMRS* (both copies)*, copBAC* and *nrsBAC* operons (Table 2). As expected from data in Figure 1, neither *petE* nor *petJ* were differentially expressed in PETR or PETP strains (Figure S7). Furthermore, *slr0601* and *slr0602* were not detected as differentially regulated in PETR or PETP (Table 2). When gene expression was directly compared between WT and PETR strains, 8 genes were differentially regulated in BG11c- Cu (7 expressed at higher levels in WT, 1 down-regulated) and 6 after copper addition (Supplementary material S3). As expected, this group of genes included *petRP* (induced 5.93 and 4.73 -fold for *petR* and 37 and 38 -fold for *petP* in BG11C-Cu and +Cu, respectively), *petE* (repressed 41-fold in -Cu and 2-fold in +Cu) and *petJ* (induced 168-fold in -Cu and 8.7-fold in +Cu) but also *slr0601*, *slr0602*, *slr0242*, *sll1796*, *sll0494* and *slr1896* (Supplementary material S4). Similarly, when WT was compared to PETP only 3 genes were differentially regulated in BG11C-Cu (all up-regulated) and 8 genes in BG11C+Cu (also up-regulated). These genes included *petP* (up-regulated 5-fold in both conditions in WT), *petE* (also up-regulated in WT (5.3-fold in -Cu and 116-fold in +Cu), *petJ* (repressed 25-fold in +Cu) and *slr0242*, *slr0601*, *slr0602*, *slr1896* and *sll1926* (Supplementary material S4). These results suggest that the PetRP regulon comprises *petJ*, *petE*, *slr0601* and *slr0602* as these genes were regulated by copper in WT and affected in both PETR and PETP strains, although with opposite patterns in the mutant strains. *slr0601* and *slr0602* are linked in the genome probably forming an operon (Figure S8a). Expression of *slr0601* was

analysed by northern blot and the expression was similar to *petJ*: repressed after copper addition in WT, not expressed in a PETR strain and constitutively expressed in the PETP strain (Figure S8b). Furthermore, PetR was able to bind to the promoter sequence of *slr0601* (Figure S8c) which contains a sequence matching the one identified in Figure 4 (Figure S8d). All these data support that the *petRP* regulon is only composed by *petJ*, *petE* and *slr0601-slr0602* in *Synechocystis*.

Physiological characterisation of PETR and PETP mutant strains.

All mutants generated in this study were fully segregated in BG11C and were able to grow in BG11C-Cu but considering their gene expression programs (Figures 1, 2 and S7; Table 2, supplementary material S3 and S4), growth defects were expected in different copper regimes. We have analysed growth of the PETR and PETP strains in plates with different copper availability: BG11C-Cu+BCSA (no copper), BG11C-Cu (~30 nM Cu) and BG11C (330 nM Cu). PETR was only affected in BG11C-Cu containing BCSA in a similar way to the PETJ strain, which has an interrupted *petJ* gene (Figure 5a). In contrast, the PETP strain was not affected in any condition (Figure 5), because it expresses *petJ* in all tested conditions (Figure 1). Finally, the PETE strain showed a reduced growth rate (but survived) in BG11C as previously described[24,25,39] (Figure 5a and S9). A double mutant lacking both genes (PETRP strain) was indistinguishable from the single mutant PETR (Figure 5a and S4). An analysis of the photosynthetic activity revealed that PETJ and PETR strains reached lower oxygen evolution rates (16.8±0.3 µmol min^{-1}/OD_{750nm} and 18.9±0.75 µmol min^{-1}/OD_{750nm} respectively) than WT (23±3.82 µmol min^{-1}/OD_{750nm}), PETE (24.5±2.46 µmol min^{-1}/OD_{750nm}) and PETP strains (23.2±5 µmol min^{-1}/OD_{750nm}) when cultured in BG11c-Cu+BCSA, although they saturated at the same light intensities (Figure 5b). When cultured in BG11C, the PETE strain exhibited a severe defect in oxygen evolution (reaching only 5.3±2.7 µmol min^{-1}/OD_{750nm} and saturating at 180 µmol $m^{-2}s^{-1}$of light intensity (Figure 5c). Surprisingly the PETP strain showed a lower maximum capacity reaching only 13.24±2.63 µmol min^{-1}/OD_{750nm} although it saturated at the same light intensity of the WT (24.11±3.66 µmol min^{-1}/OD_{750nm}), PETJ (22.25±4.34 µmol min^{-1}/OD_{750nm}) or PETR mutant (21.87±4.36 µmol min^{-1}/OD_{750nm}) (Figure 5c). The PETP strain expresses *petJ* constitutively (Figure 1), and therefore it was not expected to show any photosynthetic defect, suggesting that $Cytc_6$ might not be as efficient as PC in our culture conditions *in vivo*.

Genetic interaction between *petRP*, *petJ* and *petE*.

Our results show that *petRP* is the main system responsible for the *petJ*/*petE* switch after copper addition. Either *petJ* or *petE* are required for PSI reduction and therefore for growth of cyanobacteria[39], despite early studies showing growth of *Synechocystis* in the absence of both proteins[40]. The data presented in Figures 1 and 5 suggest that the low levels of PC present in BG11C-Cu (even in the presence of BCSA) were enough to sustain growth of PETR and PETJ mutant strains but at reduced rates (Figure 5a). Furthermore, although the PETE strain showed impaired growth in the presence of copper (Figure 5a), it was able to grow at reduced rates as all cells grew after prolonged incubation (Figure S9), probably due to low levels of $Cytc_6$. Moreover, a double mutant lacking functional *petE* and *petR* genes (or both *petR* and *petP*, strain PETERP) could not be completely segregated (Figure 6b), probably due to the low expression levels of *petJ* in the absence of PetR (Figures 1a and S7), reinforcing the idea that at least one of the soluble transporters (even at low levels) is needed in *Synechocystis*. In contrast, a double mutant lacking *petE* and *petP* (PETEP) was able to grow almost at WT rates in the presence of copper (Figure 6c and Figure S9). In close agreement, a double mutant PETJP did not segregate while PETJR and PETJRP mutants were fully segregated (Figure 6b). All these data suggested that a double mutant lacking both *petJ* and *petE* should not be viable. To test this hypothesis, a double mutant was generated by transforming the PETE mutant with the pPETJCm. Merodiploids colonies were obtained but never segregated completely (Figure S10), despite sub-culturing them in several light regimes for more than 2 years. To confirm that PC and $Cytc_6$ were expressed in slow growing mutants, we have used concentrated extracts and 150 µg of total protein were loaded per lane. $Cytc_6$ was detected at low levels in WT and PETE strains, but not in the PETR strain, in the presence of copper (Figure 6d). In WT, PETR and PETJ strains, PC is detected (although at low levels, Figures 1, 2 and 6e) in the absence of Cu, therefore allowing growth of these strains at reduced rates (Figure 5).

Discussion

Acquisition of PC as an alternative electron carrier was probably an early adaptation after oxygenic photosynthesis appeared as local oxygenation (even before GEO) probably decreased Fe availability. This is reinforced by the presence of both electron carriers in early branching cyanobacteria such as *Gloeobacter* and *Pseudoanabaena* (Figure S1). Although known for more than 40 years [12,13], the regulatory system responsible for *petE*/*petJ* switch in cyanobacteria remained undiscovered. Here we

show that *petRP* are responsible for this regulation. This hypothesis is also supported by phylogenetic distribution of *petRP*. The system seems to be early acquired during evolution, probably together with *petE* genes since is widely distributed along cyanobacteria groups and seem to be lost in those groups in which *petE* is not present or are under gene lost-driven selection (Figure S1). This is the case of *Synechococcus*/*Prochlorococcus* clade in which most of the strains have lost *petRP* similary to what also happened with other regulatory systems[41]. We have shown that *petRP* act in a single pathway in which PetR positively regulates *petJ* and negatively *petE*, while PetP regulates PetR protein levels in response to copper (Figure 7). PetR directly regulates *petE* and *petJ* gene expression by binding to the promoter regions of these two genes (Figure 4a). However, the affinity for both promoters is remarkably different, with *petJ* promoter requiring higher PetR concentrations for binding than *petE* promoter *in vitro*. Our data suggest that PetR binding to these two promoters might be in different configurations: inverted repeats in *petE* (Figure 4), where it acts as a repressor in agreement with BlaI and MecI binding to their known sequences, and direct repeats in *petJ* where it will activate transcription (Figures 1, 4 and S7). Binding to *petJ* promoter could be mediated by a higher order complex as two dimers binding to both sides of DNA, generating a structure able to activate transcription. Despite this, single complexes were detected after PetR binding to *petJ* or *slr0601* promoters (Figures 4 and S7) although with lower affinity when compared to *petE* promoter. BlaI and MecI monomer-to-dimer changes have been shown to depend on the concentration, which influences binding to DNA [42–45]. Given that the protein abundance of PetR *in vivo* depends on copper concentration (Figure 2), *petJ* will be only fully activated when all copper is exhausted, preventing induction of *petJ* if there is still some copper available for PC synthesis. Although BlaI/CopY homologs have been described to act only as repressors, our data strongly suggest that PetR acts as an activator for *petJ* expression (Figures 1, 4, S7; Table 2). This opens the possibility that BlaI/CopY homologs could also act as activators which have been also suggested previously [46]. As binding sites for PetR activation were different to repressor sites (Figure 4), it is possible that those have been elusive when PetR homologs were studied [47]. This dual role for DNA binding proteins that were initially considered as repressors has been uncovered recently in some proteins such as Fur, which was described as an activator in its apo- and holo- forms [48–50]. Our RNA-seq analysis revealed that only 4 genes are under the control of the *petRP* system in *Synechocystis*: *petE*, *petJ*, *slr0601* and *slr0602* (Table 2). *slr0601* and *slr0602* are probably forming a single transcriptional unit[51] (Figure S7). We have confirmed that *slr0601* is controlled by *petRP* using northern blot and that PetR binds to its own promoter (Figure S8).

Inspection of the promoter sequence show conservation of the core sequence identified using *petJ* and *petE* promoters GACN$_5$GTC, but also the sequences identified using only *petJ* promoters (Figure 4). This confirms that this extended sequence is probably necessary for transcriptional activation by PetR. PetP belongs to M46 family of proteases and we have shown that this protein regulates PetR by controlling its protein abundance in response to copper. This regulation is probably direct as we have shown that recombinant PetR is degraded *in vitro* by both *Synechocystis* and *E. coli* extracts and that this degradation depends on the presence of PetP and copper (Figure 3).

Furthermore, our data show that *Synechocystis* is able to synthesise PC even when copper levels are minimal due to the presence of BCSA. This indicates that some copper can be transported even in the presence of BCSA, suggesting that the copper import system (which still remains unidentified) has a higher affinity for copper than the chelating agent. This is only observed in a PETR strain in which *petE* expression is constitutive (Figures 1, 7 and S7) because in a WT strain *petE* is repressed and PC can not be synthesised even when copper is available. Finally, our data also suggest that there are other layers of regulation at posttranscriptional levels as Cytc$_6$ and PC not always correlate with mRNA levels. PC levels were higher in Cu containing media in the PETR strain in which the mRNA level of this gene does not change in response to copper (Figure 1). Similarly, Cytc$_6$ levels are reduced in a PETP strain after copper addition even if the mRNA level is not decreased. PC protein levels can be related to the protein not being correctly translated and/or folded in the absence of available copper or degradation of the apoprotein, but synthesis of Cytc$_6$ should not be altered by copper. It has been proposed that IsaR sRNA regulates *petJ* translation in response to Fe deprivation. We have not detected *isaR* as differentially regulated in our RNA-seq (Figure S11) and therefore is unlikely that this regulation is mediated by it. Finally, although single mutants in either *petJ* or *petE* are able to grow, even in the copper regime in which expression of the other gene is repressed, these strains exhibited growth and photosynthesis defects (Figure 5, 6 and S9) in agreement with previous studies[39,55–57]. Double mutants in both *petJ* and *petE* were not viable (Figure S9) and double mutants lacking one of these genes and with decreased expression of the other due to the lack of *petP* (constitutive repression of *petE*) or *petR* (unable to induce *petJ*) were not viable neither (Figure 6 and 7). All these data demonstrate that *petRP* are essential for expression of these genes and that the levels of PC or Cytc$_6$ proteins can not be below a critical threshold for survival of the strains. These results also rule out the existence of another electron transfer mechanism between cytochrome b$_6$f and PSI.

Acknowledgments.

We thank Jose Luis Crespo, Manuel J. Mallén, Miguel Roldán and Sandra Díaz-Troya for critical reading the manuscript. This research was funded by Ministerio de Economía y Competividad (MINECO) grant number BIO2016-75634-P, and by Junta de Andalucía Group BIO-284, co-financed by European Regional Funds (FEDER) to Francisco J. Florencio. RMGC is the recipient of a predoctoral contract from Ministerio de Educación, Cultura y Deporte, Spain (contract #FPU2015/05025)

References

1. Schirrmeister, B. E., de Vos, J. M., Antonelli, A. & Bagheri, H. C. Evolution of multicellularity coincided with increased diversification of cyanobacteria and the Great Oxidation Event. *Proc. Natl. Acad. Sci. U. S. A.* **110**, 1791–6 (2013).

2. Koehler, M. C., Buick, R., Kipp, M. A., Stüeken, E. E. & Zaloumis, J. Transient surface ocean oxygenation recorded in the □2.66-Ga Jeerinah Formation, Australia. *Proc. Natl. Acad. Sci. U. S. A.* **115**, 7711–7716 (2018).

3. Fischer, W. W., Hemp, J. & Johnson, J. E. Evolution of Oxygenic Photosynthesis. *Annu. Rev. Earth Planet. Sci.* **44**, 647–683 (2016).

4. Alcott, L. J., Mills, B. J. W. & Poulton, S. W. Stepwise Earth oxygenation is an inherent property of global biogeochemical cycling. *Science (80-.).* **366**, 1333–1337 (2019).

5. Hamilton, T. L. The trouble with oxygen: The ecophysiology of extant phototrophs and implications for the evolution of oxygenic photosynthesis. *Free Radical Biology and Medicine* **140**, 233–249 (2019).

6. Fischer, W. W., Hemp, J. & Valentine, J. S. How did life survive Earth's great oxygenation? *Current Opinion in Chemical Biology* **31**, 166–178 (2016).

7. Ilbert, M. & Bonnefoy, V. Insight into the evolution of the iron oxidation pathways. *Biochimica et Biophysica Acta - Bioenergetics* **1827**, 161–175 (2013).

8. Crichton, R. R. *Biological inorganic chemistry□: a new introduction to molecular structure and function* . (Academic Press, 2019).

9. Behrenfeld, M. J. & Kolber, Z. S. Widespread iron limitation of phytoplankton in

the south pacific ocean. *Science (80-.).* **283**, 840–843 (1999).

10. Finazzi, G., Sommer, F. & Hippler, M. Release of oxidized plastocyanin from photosystem I limits electron transfer between photosystem I and cytochrome b6f in vivo. *Proc. Natl. Acad. Sci. U. S. A.* **102**, 7031–7036 (2005).

11. Weigel, M. *et al.* Plastocyanin is indispensable for photosynthetic electron flow in *Arabidopsis thaliana*. *J. Biol. Chem.* **278**, 31286–9 (2003).

12. Sandmann, G. & Böger, P. Copper-induced exchange of plastocyanin and cytochrome c-533 in cultures of *Anabaena variabilis* and *Plectonema boryanum*. *Plant Sci. Lett.* **17**, 417–424 (1980).

13. Sandmann, G. Formation of plastocyanin and cytochrome c-553 in different species of blue-green algae. *Arch. Microbiol.* **145**, 76–79 (1986).

14. WOOD, P. M. Interchangeable Copper and Iron Proteins in Algal Photosynthesis: Studies on Plastocyanin and Cytochrome c□552 in Chlamydomonas. *Eur. J. Biochem.* **87**, 9–19 (1978).

15. Kropat, J. *et al.* A regulator of nutritional copper signaling in *Chlamydomonas* is an SBP domain protein that recognizes the GTAC core of copper response element. *Proc. Natl. Acad. Sci. U. S. A.* **102**, 18730–18735 (2005).

16. Sommer, F. *et al.* The CRR1 nutritional copper sensor in chlamydomonas contains two distinct metal-responsive domains. *Plant Cell* **22**, 4098–4113 (2010).

17. Zhang, L., McSpadden, B., Pakrasi, H. B. & Whitmarsh, J. Copper-mediated regulation of cytochrome c553 and plastocyanin in the cyanobacterium *Synechocystis* 6803. *J Biol Chem* **267**, 19054–19059 (1992).

18. Ghassemian, M., Wong, B., Ferreira, F., Markley, J. L. & Straus, N. A. Cloning, sequencing and transcriptional studies of the genes for cytochrome c-553 and plastocyanin from *Anabaena* sp. PCC 7120. *Microbiology* **140 (Pt 5**, 1151–9 (1994).

19. Van der Plas, J. *et al.* The gene for the precursor of plastocyanin from the cyanobacterium *Anabaena* sp. PCC 7937: isolation, sequence and regulation. *Mol. Microbiol.* **3**, 275–84 (1989).

20. Briggs, L. M., Pecoraro, V. L. & McIntosh, L. Copper-induced expression, cloning, and regulatory studies of the plastocyanin gene from the

cyanobacterium *Synechocystis* sp. PCC 6803. *Plant Mol. Biol.* **15**, 633–42 (1990).

21. Buikema, W. J. & Haselkorn, R. Expression of the *Anabaena* hetR gene from a copper-regulated promoter leads to heterocyst differentiation under repressing conditions. *Proc. Natl. Acad. Sci. U. S. A.* **98**, 2729–2734 (2001).

22. Tous, C., Vega-Palas, M. A. & Vioque, A. Conditional expression of RNase P in the cyanobacterium *Synechocystis* sp. PCC6803 allows detection of precursor RNAs. Insight in the in vivo maturation pathway of transfer and other stable RNAs. *J Biol Chem* **276**, 29059–29066 (2001).

23. Georg, J. *et al.* Acclimation of Oxygenic Photosynthesis to Iron Starvation Is Controlled by the sRNA IsaR1. *Curr. Biol.* **27**, 1425-1436.e7 (2017).

24. Giner-Lamia, J. *et al.* The CopRS Two-Component System Is Responsible for Resistance to Copper in the Cyanobacterium *Synechocystis* sp. PCC 6803. *Plant Physiol.* **159**, 1806–1818 (2012).

25. Giner-Lamia, J., López-Maury, L. & Florencio, F. J. F. J. Ni interferes in the Cu-regulated transcriptional switch *petJ/petE* in Synechocystis sp. PCC 6803. *FEBS Lett.* **590**, 3639–3648 (2016).

26. Giner-Lamia, J., López-Maury, L. & Florencio, F. J. F. J. Global transcriptional profiles of the copper responses in the cyanobacterium *Synechocystis* sp. PCC 6803. *PLoS One* **9**, e108912 (2014).

27. Liu, T. *et al.* A novel cyanobacterial SmtB/ArsR family repressor regulates the expression of a CPx-ATPase and a metallothionein in response to both Cu(I)/Ag(I) and Zn(II)/Cd(II). *J. Biol. Chem.* **279**, 17810–8 (2004).

28. García-Domínguez, M. & Florencio, F. J. Nitrogen availability and electron transport control the expression of *glnB* gene (encoding PII protein) in the cyanobacterium *Synechocystis* sp. PCC 6803. *Plant Mol. Biol.* **35**, 723–734 (1997).

29. J.F., S. & Russell, D. *Molecular Cloning: A Laboratory Manual (3-Volume Set)*. *Cold Springs Harbour Press* **1**, (2001).

30. Giner-Lamia, J. J., López-Maury, L., Florencio, F. J., L??pez-Maury, L. & Florencio, F. J. CopM is a novel copper-binding protein involved in copper resistance in *Synechocystis* sp. PCC 6803. *Microbiologyopen* **4**, 167–185 (2015).

31. Langmead, B. & Salzberg, S. L. Fast gapped-read alignment with Bowtie 2. *Nat. Methods* **9**, 357–359 (2012).

32. Anders, S., Pyl, P. T. & Huber, W. Genome analysis HTSeq-a Python framework to work with high-throughput sequencing data. **31**, 166–169 (2015).

33. Love, M. I., Huber, W. & Anders, S. Moderated estimation of fold change and dispersion for RNA-seq data with DESeq2. *Genome Biol.* **15**, (2014).

34. Shih, P. M. *et al.* Improving the coverage of the cyanobacterial phylum using diversity-driven genome sequencing. *Proc. Natl. Acad. Sci. U. S. A.* **110**, 1053–1058 (2013).

35. Nguyen, L.-T., Schmidt, H. A., Von Haeseler, A. & Minh, B. Q. IQ-TREE: A Fast and Effective Stochastic Algorithm for Estimating Maximum-Likelihood Phylogenies. doi:10.1093/molbev/msu300

36. Letunic, I. & Bork, P. Interactive Tree Of Life (iTOL) v4: recent updates and new developments. *Web Serv. issue Publ. online* **47**, (2019).

37. Giner-Lamia, J., López-Maury, L. & Florencio, F. J. CopM is a novel copper-binding protein involved in copper resistance in *Synechocystis* sp. PCC 6803. *Microbiologyopen* **4**, (2015).

38. Peacock, S. J. & Paterson, G. K. Mechanisms of Methicillin Resistance in *Staphylococcus aureus*. *Annu. Rev. Biochem.* **84**, 577–601 (2015).

39. Durán, R. V, Hervás, M., De La Rosa, M. A. & Navarro, J. A. The efficient functioning of photosynthesis and respiration in *Synechocystis* sp. PCC 6803 strictly requires the presence of either cytochrome c6 or plastocyanin. *J. Biol. Chem.* **279**, 7229–33 (2004).

40. Zhang, L., Pakrasi, H. B. & Whitmarsh, J. Photoautotrophic growth of the cyanobacterium *Synechocystis* sp. PCC 6803 in the absence of cytochrome c553 and plastocyanin. *J Biol Chem* **269**, 5036–5042 (1994).

41. Lambrecht, S. J., Steglich, C. & Hess, W. R. A minimum set of regulators to thrive in the ocean. *FEMS Microbiol. Rev.* (2020). doi:10.1093/femsre/fuaa005

42. Filée, P. *et al.* Dimerization and DNA binding properties of the *Bacillus licheniformis* 749/I BlaI repressor. *J. Biol. Chem.* **278**, 16482–7 (2003).

43. Blázquez, B. *et al.* Regulation of the expression of the β-lactam antibiotic-resistance determinants in methicillin-resistant *Staphylococcus aureus* (MRSA).

Biochemistry **53**, 1548–1550 (2014).

44. Llarrull, L. I., Prorok, M. & Mobashery, S. Binding of the gene repressor BlaI to the bla operon in methicillin-resistant *Staphylococcus aureus*. *Biochemistry* **49**, 7975–7 (2010).

45. Boudet, J. *et al.* Conformational and thermodynamic changes of the repressor/DNA operator complex upon monomerization shed new light on regulation mechanisms of bacterial resistance against b-lactam antibiotics. *Nucleic Acids Res.* **35**, 4384–4395 (2007).

46. Pence, M. A. *et al.* Beta-lactamase repressor BlaI modulates *Staphylococcus aureus* cathelicidin antimicrobial peptide resistance and virulence. *PLoS One* **10**, (2015).

47. Sala, C. *et al.* Genome-wide regulon and crystal structure of BlaI (Rv1846c) from *Mycobacterium tuberculosis*. *Mol. Microbiol.* **71**, 1102–16 (2009).

48. Seo, S. W. *et al.* Deciphering Fur transcriptional regulatory network highlights its complex role beyond iron metabolism in *Escherichia coli*. *Nat. Commun.* **5**, 4910 (2014).

49. Pinochet-Barros, A. & Helmann, J. D. Bacillus subtilis Fur is a transcriptional activator for the PerR-repressed *pfeT* gene encoding an iron efflux pump. *J. Bacteriol.* (2020). doi:10.1128/JB.00697-19

50. Delany, I., Rappuoli, R. & Scarlato, V. Fur functions as an activator and as a repressor of putative virulence genes in *Neisseria meningitidis*. *Mol. Microbiol.* **52**, 1081–1090 (2004).

51. Mitschke, J. *et al.* An experimentally anchored map of transcriptional start sites in the model cyanobacterium *Synechocystis* sp. PCC6803. *Proc. Natl. Acad. Sci. U. S. A.* **108**, 2124–2129 (2011).

52. Belluzo, B. S. *et al.* An experiment-informed signal transduction model for the role of the *Staphylococcus aureus* MecR1 protein in β-lactam resistance. *Sci. Rep.* **9**, 19558 (2019).

53. Llarrull, L. I., Toth, M., Champion, M. M. & Mobashery, S. Activation of BlaR1 protein of methicillin-resistant *Staphylococcus aureus*, its proteolytic processing, and recovery from induction of resistance. *J. Biol. Chem.* **286**, 38148–38158 (2011).

54. Staude, M. W. *et al.* Investigation of signal transduction routes within the sensor/transducer protein BlaR1 of *Staphylococcus aureus*. *Biochemistry* **54**, 1600–10 (2015).

55. Wang, X.-Q., Jiang, H.-B., Zhang, R. & Qiu, B.-S. Inactivation of the *petE* gene encoding plastocyanin causes different photosynthetic responses in cyanobacterium *Synechocystis* PCC 6803 under light-dark photoperiod and continuous light conditions. *FEMS Microbiol. Lett.* **341**, 106–114 (2013).

56. Ardelean, I., Matthijs, H. C. ., Havaux, M., Joset, F. & Jeanjean, R. Unexpected changes in photosystem I function in a cytochrome c 6 -deficient mutant of the cyanobacterium *Synechocystis* PCC 6803. *FEMS Microbiol. Lett.* **213**, 113–119 (2002).

57. Ivanov, A. G. *et al.* Restricted capacity for PSI-dependent cyclic electron flow in ΔpetE mutant compromises the ability for acclimation to iron stress in *Synechococcus* sp. PCC 7942 cells. in *Biochimica et Biophysica Acta - Bioenergetics* **1817**, 1277–1284 (2012).

Table 1. *Synechocystis* strains used in this work.

STRAIN	RELEVANT GENOTYPE	Mutated ORFs	SOURCE
WT	*Synechocystis* sp. PCC 6803	-	Lab collection
PETE	*petE::C.K1*	*sll0199*	*(Giner-Lamia et al., 2012)*
PETJ	*petJ::Cm*	*sll1796*	This study
PETR	*petR::Sp*	*slr0240*	This study
PETP	*ΔpetP::Ery*	*slr0241*	This study
PETRP	*ΔpetPR::Sp*	*slr0240, slr0241*	This study
PETER	*petE::C.K1; petR::Sp*	*sll0199, slr0240*	This study
PETJR	*petJ::Cm; petR::Sp*	*sll1796, slr0240*	This study
PETEP	*petE::C.K1; ΔpetP::Ery*	*sll0199, slr0241*	This study
PETJP	*petJ::Cm; ΔpetP::Ery*	*sll1796, slr0241*	This study
PETERP	*petE::C.K1; ΔpetRP::Sp*	*sll0199, slr0240, slr0241*	This study
PETJRP	*petJ::Cm; ΔpetRP::Sp*	*sll1796, slr0240, slr0241*	This study
PETER	*petE::C.K1; petR::Sp*	*sll0199, slr0240*	This study
PETEJ	*petE::C.K1; petJ::Cm*	*sll0199, sll1796*	This study

Table 2. Differentially regulated genes (P_{adj} <0.01, 2- fold change (n= 3)) identified in WT, PETR and PETP strains after copper addition. NS: not significant; repressed genes are expressed as negative fold change.

systematic ID	Fold Change WT	Fold Change PETR	Fold Change PETP	Gene name	Annotation
sll0199	24.28	NS	NS	*petE*	plastocyanin
sll0788	9.40	10.88	9.06	*copM*	copper binding protein involves in copper resistance; chromosomal copy
sll0789	16.58	18.35	31.88	*copR, rre34*	two-component response regulator OmpR subfamily involved in copper resistance; chromosomal copy
sll0790	6.16	5.00	8.08	*hik31, copS*	two-component sensor histidine kinase involved in copper resistance; chromosomal copy
sll1796	-16.66	NS	NS	*petJ*	cytochrome c_6
slr0601	-5.55	NS	NS	*slr0601*	unknown protein
slr0602	-2.32	NS	NS	*slr0602*	unknown protein
slr0793	6.50	13.51	9.34	*nrsB*	cation efflux system protein involved in nickel and cobalt tolerance
slr0794	4.29	5.66	5.01	*nrsA*	cation efflux system protein involved in nickel and cobalt tolerance
slr0795	5.10	5.46	7.46	*nrsC*	cation efflux system protein involved in nickel and cobalt tolerance
slr6039	11.75	14.26	11.98	*pcopM, hypoP*	copper binding protein involves in copper resistance; plasmid copy
slr6040	16.16	16.19	40.61	*pcopR, rreP*	two-component response regulator OmpR subfamily involved in copper resistance; plasmid copy
slr6041	10.20	7.53	9.07	*pcopS, hikP,*	two-component sensor histidine kinase involved in copper resistance; plasmid copy
slr6042	18.47	21.36	27.93	*copB*	cation efflux system protein involved in copper tolerance; czcB homolog
slr6043	17.30	23.26	29.62	*copA*	cation efflux system protein involved in copper tolerance; czcA

					homolog
slr6044	9.56	14.28	16.85	*copC*	cation efflux system protein involved in copper tolerance;
slr6045	4.37	6.13	6.20	*slr6045*	unknown protein
slr0145	NS	-2.44	NS	*slr0145*	unknown protein
slr0917	NS	NS	-2.0	*bioF*	7-keto-8-aminopelargonic acid synthetase

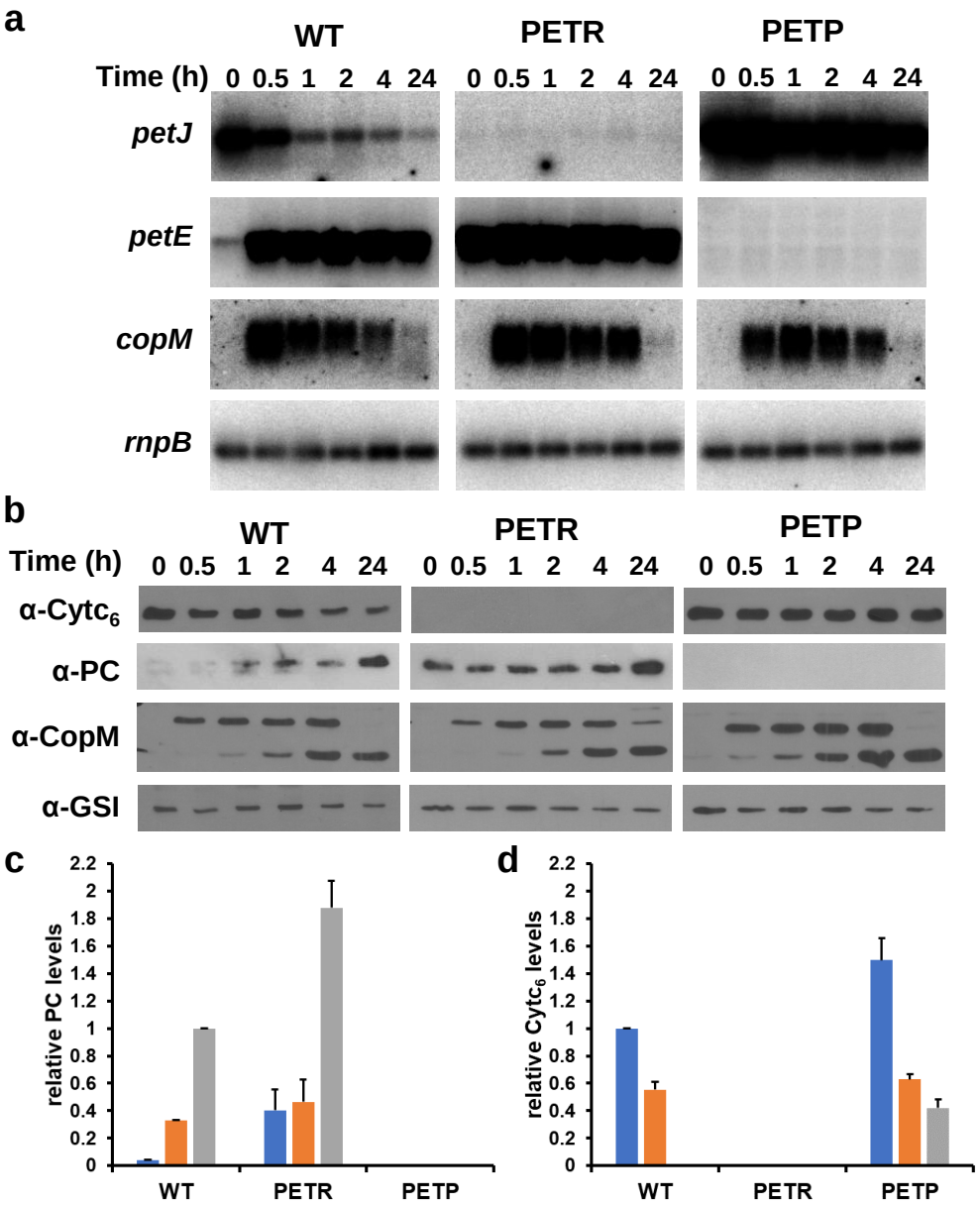

Figure 1. PetRP regulatory system controls *petJ*/*petE* switch in *Synechocystis* sp. PCC 6803.

a. Northern blot analysis of *petE*, *petJ* and *copM* in WT, PETR and PETP strains in response to 0.5 µM copper addition. Total RNA was isolated from cells grown in BG11C-Cu medium at the indicated times after addition of 0.5 µM of copper. The filters were hybridized with *petJ*, *petE* and *copM* probes and subsequently stripped and re-hybridized with a *rnpB* probe as a control.

b. Western blot analysis of PC, $Cytc_6$, CopM and GSI in WT, PETR and PETP strains in response to 0.5 µM copper addition. Cells were grown in BG11C-Cu medium and cells were harvested at the indicated times addition of 0.5 µM of copper. 5 µg of total protein from soluble extracts was separated by 15 % SDS-PAGE and subjected to western blot to detect PC, $Cytc_6$,CopM or GSI.

c. Quantification of PC levels in WT, PETR and PETP strains grown in BG11c-Cu +BCSA (blue bars), BG11C-Cu (orange bars) or BG11C (grey bars). 10 µg of total soluble proteins were loaded and compared to serial dilutions (100%, 50%, 25% and 12.5%) of the WT extract prepared from cells grown in BG11C. Data are the mean ± SE of three biologically independent experiments.

d. Quantification of $Cytc_6$ levels in WT, PETR and PETP strains grown in BG11c-Cu +BCSA (blue bars), BG11C-Cu (orange bars) or BG11C (grey bars). 10 µg of total soluble proteins were loaded and compared to serial dilutions (100%, 50%, 25% and 12.5%) of the WT extract prepared from cells grown in BG11C-Cu+BCSA. Data are the mean ± SE of three biologically independent experiments.

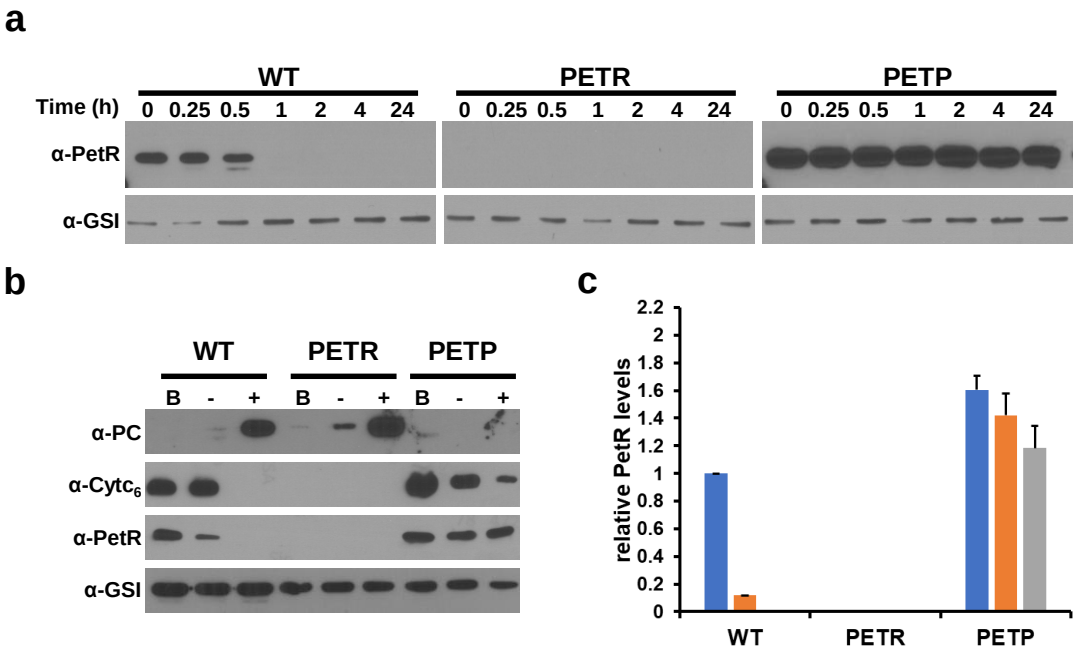

Figure 2. PetP regulates PetR levels in response to copper.

a. Western blot analysis of PetR in WT, PETR and PETP strains in response to 0.5 µM copper addition. Cells were grown in BG11C-Cu medium and harvested at the indicated times after addition of 0.5 µM of copper. Whole cells were loaded (0.2 OD_{750nm}), separated by 15 % SDS-PAGE and subjected to western blot to detect PetR or GSI as loading control.

b. Western blot analysis of $Cytc_6$, PC and PetR in WT, PETR and PETP strains grown BG11C-Cu+BCSA (B), BG11C-Cu (-) or BG11C. 10 µg of total soluble proteins were separated by 15 % SDS-PAGE and subjected to western blot to detect PC, $Cytc_6$, or GSI as loading control. For PetR whole cell extracts were used and 20 µl (equivalent to 0.2 OD_{750nm}) were loaded per lane.

c. Quantification of PetR levels in WT, PETR and PETP strains grown in BG11C-Cu +BCSA (blue bars), BG11C-Cu (orange bars) or BG11C (grey bars). 20 µl of the whole cells extract were loaded and compared to serial dilutions (100%, 50%, 25% and 12.5%) of the WT extract prepared from cells grown in BG11C-Cu+BCSA. Data are the mean ± SE of three biologically independent experiments.

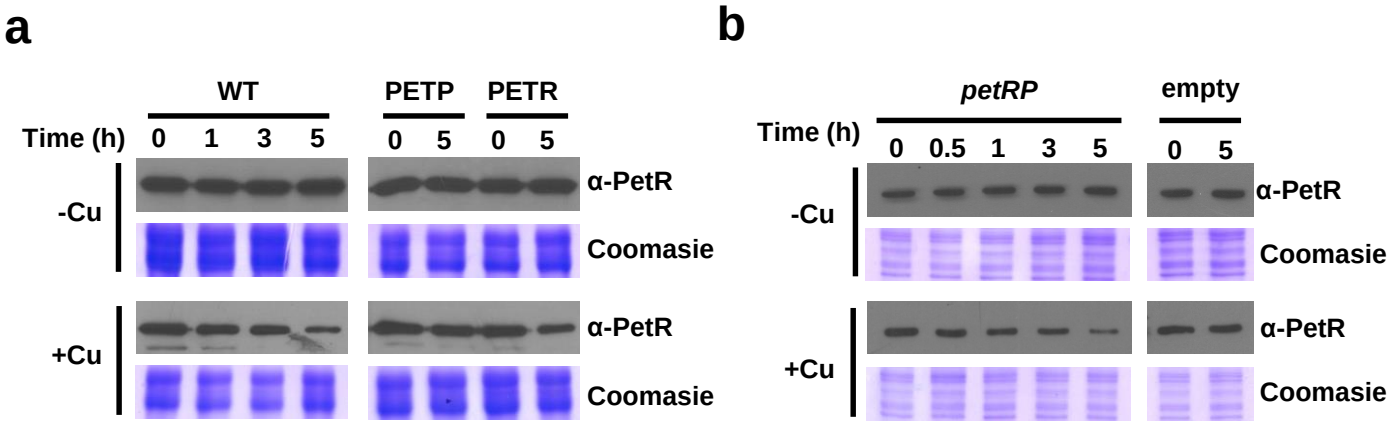

Figure 3. PetP is a copper activated protease that degrades PetR.

a. GST-PetR was incubated for the indicated time with total extracts prepared from WT, PETR and PETP strains grown in BG11C-Cu. 0.5 µM $CuSO_4$ was added to the extracts as indicated. Samples were taken at the indicated times, mixed with Laemmli buffer, boiled, separated in 12% SDS-PAGE gels and GST-PetR was detected using PetR antibodies.

b. GST-PetR was incubated for the indicated time with whole cell extracts prepared from *E. coli* carrying pN_petRP or pN_Nat (an empty plasmid) grown in M9 minimal media. 0.5 µM $CuSO_4$ was added to the extracts as indicated. Samples were taken at the indicated times, mixed with Laemmli buffer, boiled, separated in 12% SDS-PAGE gels and GST-PetR was detected using PetR antibodies.

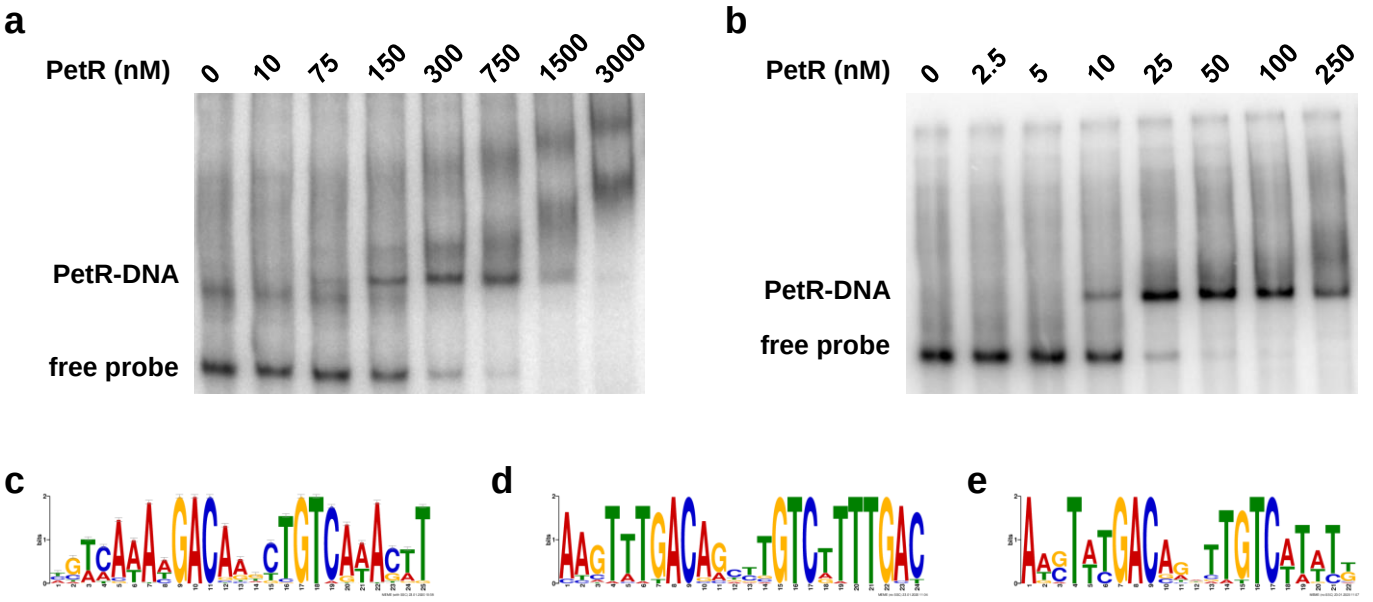

f

```
ttagcttgaccgcaactttgacagattgtcttttgactttgcctggaccgcctcccataataccttcGn34atg        petJ

                ctgaggctgtataatctacgacgggctgtcaaacattgtgataccatgggcagAn96atg        petE
```

Figure 4. PetR binds to *petJ* and *petE* promoters.

a. Electrophoretic mobility shift assay using recombinant PetR to a 103 pb *petJ* promoter probe. The indicated PetR concentration were used in each lane.
b. Electrophoretic mobility shift assay using recombinant PetR to a 217 pb *petE* promoter probe. The indicated PetR concentration were used in each lane.
c. Sequence logo identified with MEME using upstream sequences (300 pb) from *petE* and *petJ* genes from genomes that also contained *petRP*.
d. Sequence logo identified with MEME using upstream sequences (300 pb) from *petJ* genes from genomes that also contained *petRP*.
e. Sequence logo identified with MEME using upstream sequences (300 pb) from *petE* from genomes that also contained *petRP*.
f. Alignment of the *petJ* and *petE* promoter sequences from *Synechocystis*. Transcriptional start sites are in capital letters and underlined, -10 boxes are yellow underlined and conserved nucleotides from the motif found in c are in red.

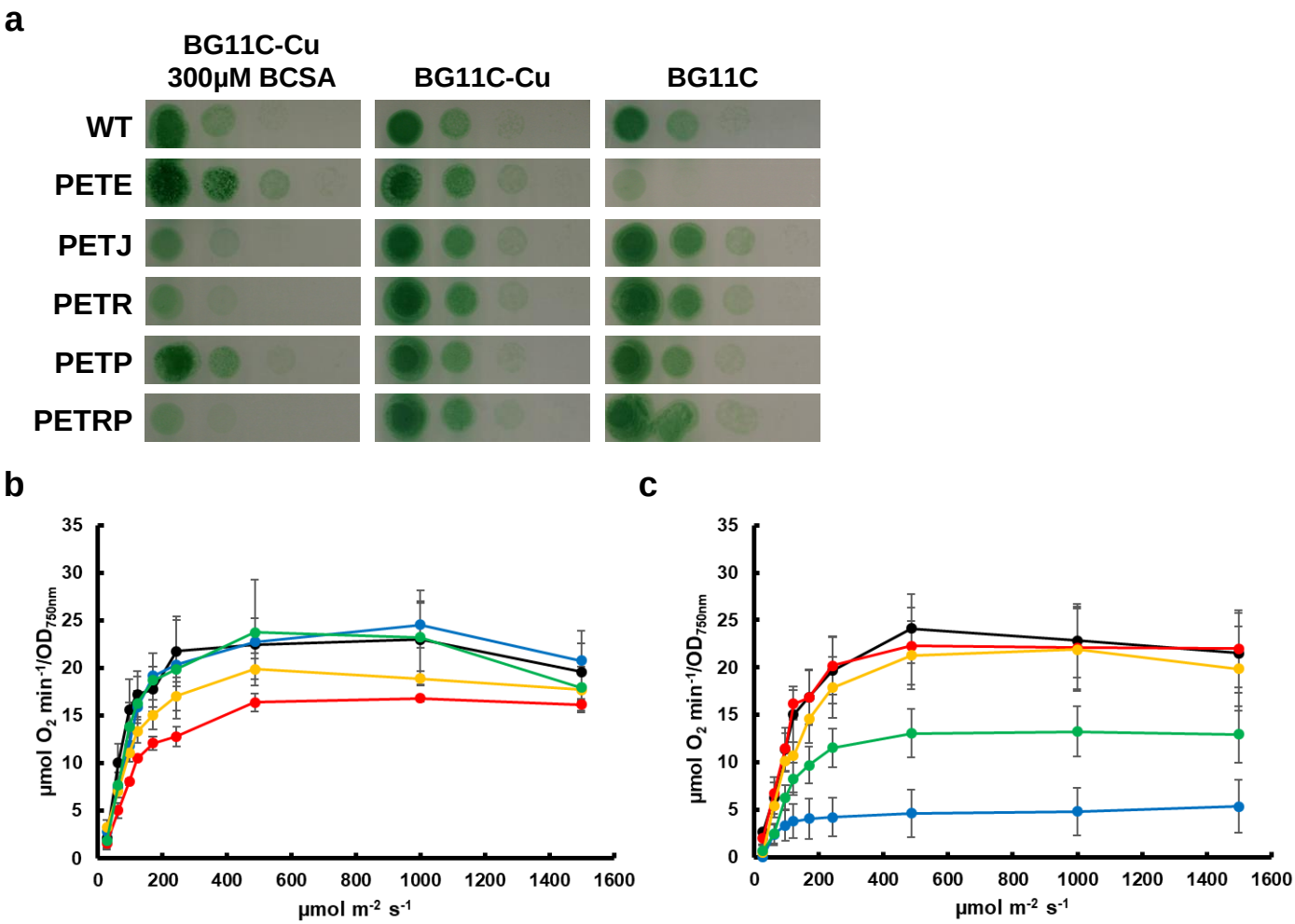

Figure 5. Physiological characterization of *petR* and *petP* mutant strains.

a. Growth of WT, PETE, PETJ, PETR, PETP and PETRP strains in different copper availability regimes. Tenfold serial dilutions of a 1 µg chlorophyll mL^{-1} cells suspension were spotted onto BG11C-Cu, BG11C-Cu o BG11C. Plates were photographed after 5 days of growth

b. Oxygen evolution measured using a Clark electrode at increasing light intensities in exponential growing cultures (OD_{750nm}= 0.5-1) of WT (●), PETJ (●), PETE (●), PETR (●) and PETP (●) strains grown in BG11C-Cu+BCSA. Data are the mean ± SE of at least three biologically independent experiments.

c. Oxygen evolution measured using a Clark electrode at increasing light intensities in exponential growing cultures (OD_{750nm}= 0.5-1) of WT (●), PETJ (●), PETE (●), PETR (●) and PETP (●) strains grown in BG11C. Data are the mean ± SE of at least three biologically independent experiments.

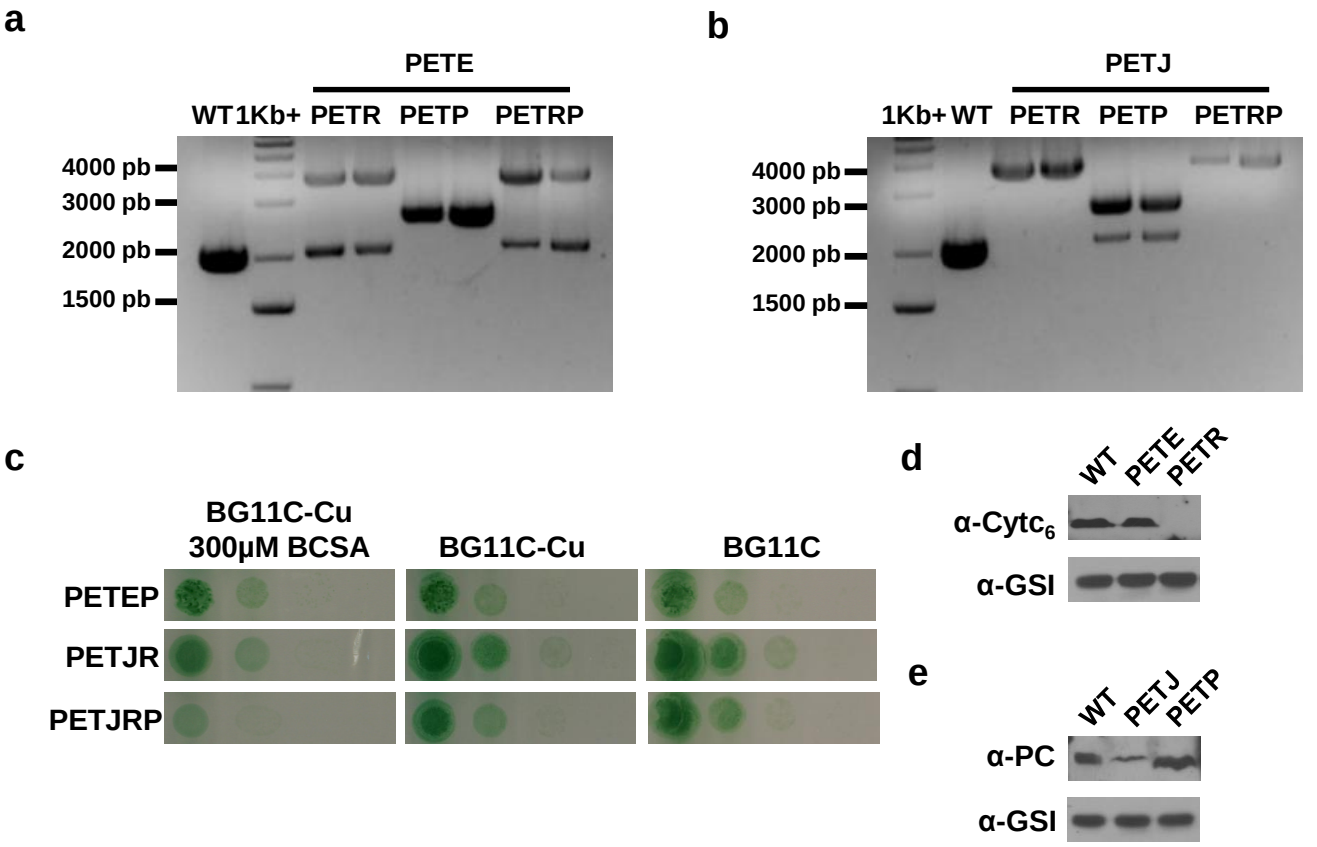

Figure 6. Genetic interactions between *petJ*, *petE* and *petRP*.

a. PCR analysis of the *petRP* locus in WT, PETER, PETEP and PETERP strains (two clones were analysed for each strain) using oligonucleotides 223-249.
b. PCR analysis of the *petRP* in WT, PETJR, PETJP and PETJRP mutant strains (two clones were analysed for each strain) using oligonucleotides 223-249.
c. Growth of PETEP, PETJR and PETJRP strains in different copper availability regimes. Tenfold serial dilutions of a 1 µg chlorophyll mL^{-1} cells suspension were spotted onto BG11C-Cu+BCSA, BG11C-Cu o BG11C. Plates were photographed after 5 days of growth.
d. Western blot analysis of $Cytc_6$ levels in WT, PETE and PETR strains. Cells were grown in BG11C medium and harvested during exponential growth (3-5 µg chl mL^{-1}). 150 µg of total protein from soluble extracts was separated by 15 % SDS-PAGE and subjected to western blot to detect $Cytc_6$ or GSI.
e. Western blot analysis of PC levels in WT, PETJ and PETP strains. Cells were grown in BG11C-Cu+BCSA medium and harvested during exponential growth (3-5 µg chl mL^{-1}). 150 µg of total protein from soluble extracts was separated by 15 % SDS-PAGE and subjected to western blot to detect PC or GSI.

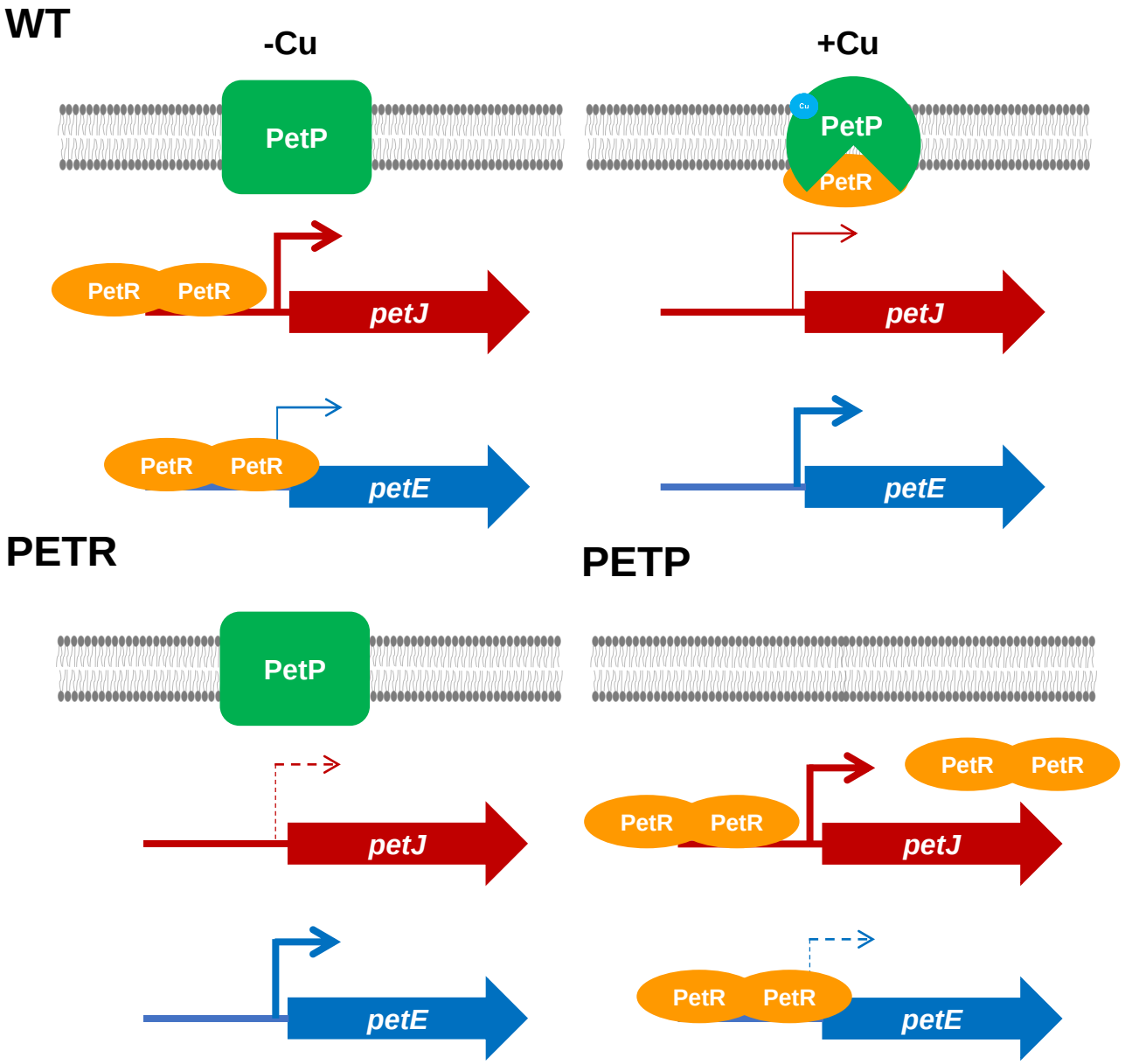

Figure 7. Model of the regulatory mechanism for *petE*/*petJ* switch mediated by PetRP.